Circular scanlines and circular windows: new tools for characterizing the geometry of fracture traces

M. Mauldon[a,*], W.M. Dunne[b], M.B. Rohrbaugh Jr.[b]

[a]*Institute for Geotechnology, Department of Civil and Environmental Engineering, University of Tennessee, Knoxville, TN 37996, USA*
[b]*Department of Geological Sciences, University of Tennessee, Knoxville, TN 37996, USA*

Abstract

We introduce new estimators for fracture trace intensity, trace density and mean trace length that exploit the use of circles as efficient sampling tools. A fracture trace is the commonly observed surface expression of a fracture, i.e. the intersection of a fracture with an exposed surface such as a rock pavement or a mine drive wall. Trace intensity, trace density and mean trace length estimators are derived and shown to form a self-consistent set of two-dimensional fracture abundance measures. The intensity estimator $n/4r$ uses the number, n, of intersections between fracture traces and a circular scanline of radius r. The density estimator $m/2\pi r^2$ uses the number, m, of trace endpoints inside a circular window. The mean trace length estimator $(n/m)\pi r/2$ uses the ratio of the number of trace intersections on the circle to the number of endpoints in the circle.

The circular sampling tools and estimators described here eliminate most sampling biases due to orientation and also correct many errors due to censoring and length bias that plague established scanline and areal measurement techniques. Performance of the estimators is demonstrated by comparison with areal samples of a synthetic fracture trace population with known intensity, density and mean trace length. The estimators are also applied successfully to a natural rock pavement with two orthogonal fracture sets, one of which is severely censored. Because the new circle-based estimators only require counts of trace–circle intersections and/or trace endpoints, they are more time-efficient than current methods for estimating geometric characteristics of fracture traces. © 2001 Elsevier Science Ltd. All rights reserved.

1. Introduction

Fractures are central to understanding rock mass strength, deformability, stability, fluid flow, contaminant transport, petroleum storage and extraction, fracture mechanisms, and tectonic history. Rock fractures typically are not directly observable in complete three-dimensional form, but rather as traces viewed on a surface such as an outcrop, rock core or mine wall. Characteristics of fractures and fracture sets are commonly inferred from fracture trace parameters such as trace density, intensity and length, taking into account the three-dimensional rock structure. Determination of the fracture trace parameters themselves, however, may be subject to significant error due to censoring and length bias on the measurement plane (Priest, 1993). In the spirit of Lord Kelvin's famous dictum that "when you can measure what you are speaking about, and express it in numbers, you know something about it", this paper presents a strategy for obtaining estimates of trace intensity, trace density and mean trace length using circular scanlines and circular windows. The focus of the paper is strictly on fracture traces; relationships between traces and the 3-d parent fracture network are not examined here (Terzaghi, 1965; Warburton, 1980a,b).

Trace intensity is defined as mean total trace length of fractures per unit area (m/m^2), *trace density* is defined as mean number of trace centers per unit area (1/m^2), and *mean trace length* is defined as the mean trace length for the individual fractures in a population (m). With respect to the above three parameters, Fig. 1 contrasts the limited view of fracture traces afforded a geologist in the field (Fig. 1a–c) with the same traces viewed by an omniscient observer (Fig. 1d–f). Summing visible lengths within the limited exposure and dividing by area (Fig. 1a, d) yields a direct unbiased estimate of trace intensity. Direct field estimates of trace density, however, may be biased because trace centers cannot always be identified (Fig. 1b vs. e). Similarly, estimates of mean trace length may be skewed because entire lengths of some traces are not visible (an effect known as censoring), and because the exposure preferentially samples longer traces (an effect known as

* Corresponding author. Fax: 00-1-865-974-2368.
E-mail address: mauldon@utk.edu (M. Mauldon).

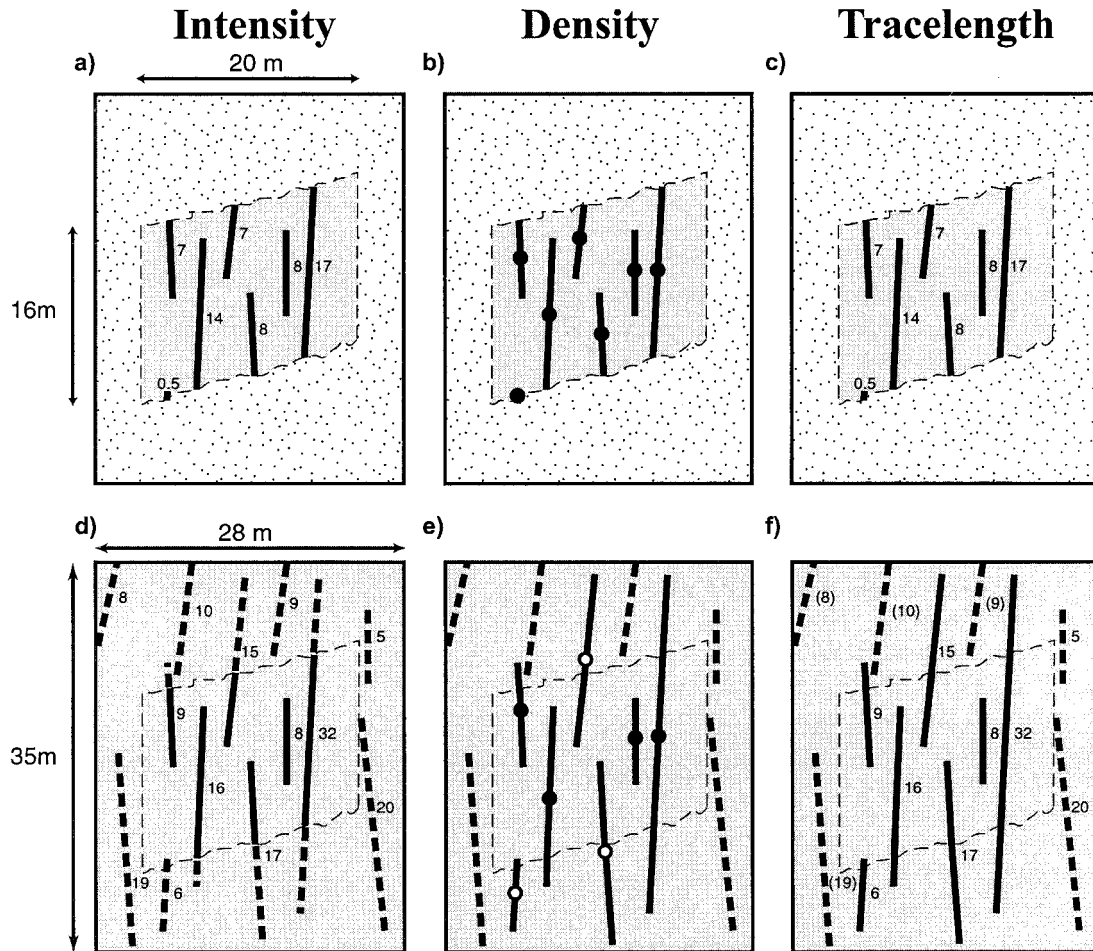# Intensity   Density   Tracelength

Fig. 1. Fracture trace characteristics and effects of sampling biases. Traces as seen in a field exposure or window (stippled area is covered). (a) Intensity (61.5 m/320 m$^2 = 0.2$ m^{-1}). (b) Apparent density ($7/320$ m$^2 = 0.02$ m^{-2}; black dots: apparent centers). (c) Apparent mean trace length (61.5 m/$7 = 8.8$ m). Traces with hidden parts exposed. (d) Intensity (174 m/980 m$^2 = 0.2$ m^{-1}; dashed lines: trace segments not visible in window). (e) True density ($4/320$ m$^2 = 0.01$ m^{-2}; white and black dots: true centers for traces that intersect window). (f) Uncensored mean trace length (103 m/$7 = 15$ m; solid lines: true lengths of traces that intersect window).

length bias; Fig. 1c vs. f). In most cases, when field data are used directly, these sampling problems result in over-estimates of trace density and underestimates of mean trace length.

This paper contains derivations of trace intensity, density and mean trace length estimators for circular scanlines and windows. While these estimators have been described individually in previous papers (Mauldon, 1998; Mauldon et al., 1999a,b), they are shown here to be mutually consistent. The trace parameters themselves are also shown to form a unified set of fracture abundance measures. Therefore, a contribution of this paper is integration of the three estimators into a unified system.

Circular scanlines and circular windows, together with new circle-based estimators, provide time-efficient estimates for trace density, intensity and mean trace length that eliminate orientation bias, censoring and length bias with respect to measurements in the plane. Circular scanlines are simply circles drawn on a rock surface, on a fracture trace map, or on a digital image. A circular window

is the region enclosed by a circular scanline. The possibility of using circular scanlines to reduce directional bias in fracture orientation measurements was mentioned previously by Baecher and Lanney (1978), Titley et al. (1986), and Davis and Reynolds (1996), but without quantitative analyses. Circular scanlines and windows, and indeed any other linear or areal measurement devices, sample an exposed rock surface, which itself represents a sample of the underlying trace population for the coincident plane. This underlying trace population is the target population for this study. Visible traces can be used to estimate the true trace population parameters if sampling biases are recognized and corrected. The strategy adopted here is to use circular scanlines and windows to *resample* the exposed traces in such a way that sampling biases are eliminated. To demonstrate the performance of the estimators, estimates using randomly placed circles are compared to known values of the parameters for a population of synthetic fracture traces. The estimators are then applied to natural fracture traces at Llantwit Major, Wales, for
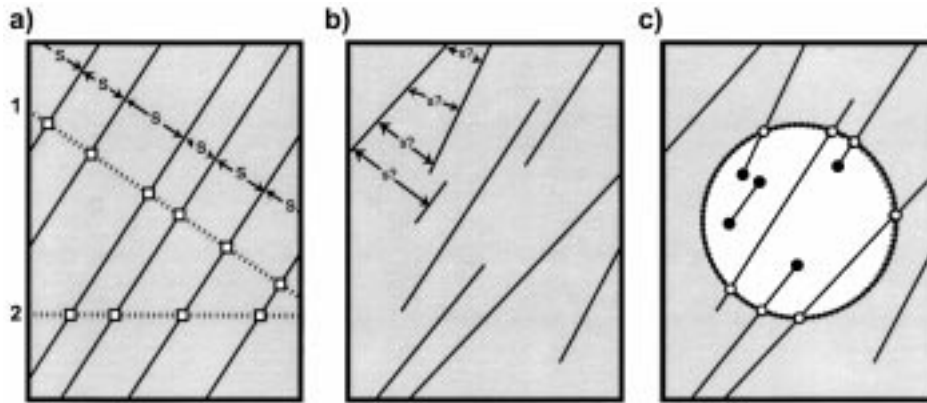
Fig. 2. Tools for sampling fracture traces. (a) Parallel persistent traces; spacing (*s*) well defined. Scanline 1: normal; scanline 2: at an arbitrary angle; shaded region: areal sample of censored traces. (b) Subparallel impersistent traces; spacing (*s*?) poorly defined. (c) Subparallel impersistent traces: circular scanline with *n* trace intersections (white dots, $n = 7$), circular window (white) with *m* trace endpoints (black dots, $m = 5$).

comparison with estimates from whole-exposure samples. Detailed discussion of the performance of the estimators as measurement tools is given in Rohrbaugh et al. (2000).

2. Background

2.1. Trace intensity

Mean spacing is easily determined for parallel persistent fractures (Fig. 2a) (Priest and Hudson, 1981; Hancock, 1985; Pollard and Aydin, 1988), but for non-parallel, subparallel or impersistent fractures the meaning of spacing is unclear (Fig. 2b). Approaches to defining and measuring spacing for such cases (Fig. 2b) include application of Terzaghi corrections to each individual feature on a randomly located scanline (Terzaghi, 1965; Priest, 1993; Mauldon and Mauldon, 1997), and calculation of an equivalent mean spacing from intensity (Dershowitz and Herda, 1992; Wu and Pollard, 1995).

Intensity, which may be thought of as the product of fracture density and mean size, is a less ambiguous measure of fracture abundance, directly applicable in its two-dimensional form to cases such as Fig. 2b. Fracture intensity (fracture area/rock volume), areal intensity (trace length/sample area) and linear intensity (fracture number/scanline length), all with dimension L^{-1}, denote intensity in three, two and one dimensions, respectively (Oda, 1993; Mauldon, 1994; Dershowitz et al., 2000), and are basic quantities of stereology (e.g. Underwood, 1970). Areal and linear intensity are functions of the orientation of the plane or line on which the intensity is measured.

For parallel persistent fractures and a normal scanline (Fig. 2a, Line 1), linear intensity, or frequency, is the reciprocal of mean spacing, and thus spacing and intensity are closely related (Priest, 1993; Mauldon, 1994; Becker and Gross, 1996). The advantages of intensity over spacing, however, are several. First, intensity is directly applicable to cases such as Fig. 2b, where spacing is poorly defined.

Second, intensities of individual sets are additive, whereas spacings are not. Third, intensity is the product of fracture density and mean trace length, if density and trace length are uncorrelated. Intensity, density and mean trace length therefore constitute a unified set of consistent fracture characteristics (Mauldon, 1994; Dershowitz et al., 2000), whereas spacing as such is an isolated parameter. Consequently, in this paper we pursue the derivation of an unbiased estimator for intensity rather than spacing.

2.2. Trace density

One way to estimate trace density would be to count the number of visible complete and partial traces and divide by window area (Fig. 1b). This operation, however, yields *apparent density*, which is scale dependent and over-estimates the actual number of traces per unit area (Fig. 1e). In contrast, true fracture trace density, defined as the number of trace centers per unit area, is scale independent but cannot be obtained directly from field data because only centers of those traces fully visible within the window are identifiable. Traces that are partially, but not fully, visible in a window are referred to as *censored*; part of the trace is restricted from view (Fig. 1b).

To circumvent the problem of unidentifiable trace centers, Kulatilake and Wu (1984a) estimated the probability, assuming a particular trace length distribution, that a window contains a given trace midpoint. The form of trace length distributions, however, lacks consensus (e.g. LaPointe, 1993; Odling, 1997) and general distributional forms may not in any case be applicable to a particular fracture pattern. This paper presents instead a distribution-free estimator for trace density, predicated on the association between trace ends and trace centers (Fig. 3).

2.3. Mean trace length

Estimation of mean trace length has received considerable attention in the rock mechanics literature and to some
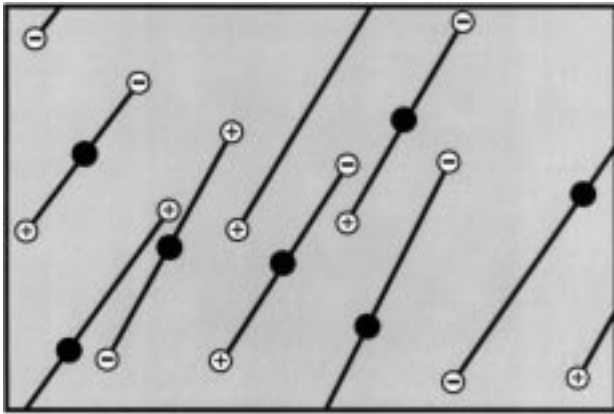
Fig. 3. Association between trace centers (black dots) and trace endpoints (white circles with randomly assigned plus or minus signs). Some centers and endpoints are concealed due to censoring.

extent in the geological and applied statistics literature, and has long been recognized as a thorny issue. With respect to estimating mean trace length, two major biases, censoring and length bias, have been identified (Epstein, 1954; Call et al., 1976; Parker and Cowan, 1976; Cruden, 1977; Baecher and Lanney, 1978; Baecher, 1980; Pahl, 1981; Priest and Hudson, 1981; Laslett, 1982; Kulatilake and Wu, 1984b; Panek, 1985; Villaescusa and Brown, 1992; Priest, 1993; Odling, 1997; Mauldon, 1998; Zhang and Einstein, 1998; Mauldon et al., 1999b). Efforts to circumvent or correct for these sampling biases include (1) methods that assume a particular form for the trace length distribution of the sampled population, and (2) methods that are distribution free (Maritz, 1981). The latter are directly applicable regardless of the underlying trace length distribution. The mean trace length estimator presented in this paper is distribution free.

2.4. Sampling methods

Fracture trace characteristics are typically gathered using linear or areal sampling techniques. Straight scanlines sample the fractures that intersect a line and may be used to record number, orientation, aperture, semi-trace length, etc., in a systematic manner (Priest and Hudson, 1981). Fracture trace data gathered with scanlines are subject to orientation, censoring and length biases. Orientation bias, introduced when a scanline is not perpendicular to a set of parallel traces (Fig. 2a, Line 2), may be reduced by applying a trigonometric correction factor (Terzaghi, 1965; Mauldon and Mauldon, 1997) to obtain an improved estimate of frequency, and hence, intensity. For non-parallel traces (Fig. 2b), such Terzaghi corrections can be applied to each encountered feature individually. Application of the trigonometric factor breaks down, however, for traces subparallel to the scanline (Terzaghi, 1965; Priest, 1993).

Areal sampling usually involves mapping the fracture pattern on a surface and recording characteristics for visible

fractures (Wu and Pollard, 1995). Use of an equant sampling area, ideally a circle, eliminates orientation bias in the plane. Typically, because areal samples comprise larger data sets than scanline samples, the effects of censoring and length bias may be less pronounced than for scanlines. Trace maps also have the advantage of recording the trace pattern, termination relationships and other aggregate properties of the areal sample (Dershowitz and Einstein, 1988). Construction of fracture trace maps for areal samples, however, tends to be very time consuming (Rohrbaugh et al., 2001, in review). Furthermore, as illustrated in Fig. 1, trace map data taken at face value can lead to highly erroneous conclusions regarding trace density and length.

Circular scanlines and windows provide an approach to estimating fracture trace parameters that exploits the time efficiency of scanlines, while automatically correcting for errors due to orientation bias, censoring and length bias. The trace intensity estimate is obtained from the number (n) of joint intersections with a circular scanline (Fig. 2c) (Mecke, 1981; Stoyan et al., 1995; Mauldon et al., 1999a). The density estimate is obtained from the number (m) of joint endpoints inside the circular window (Fig. 2c) (Mauldon, 1998; Mauldon et al., 1999b). The estimate of mean trace length is obtained from the ratio (n/m) of the number of intersections on the circle to the number of endpoints inside the circle (Fig. 2c) (Mauldon, 1998; Mauldon et al., 1999b).

Throughout this paper, statistical independence between trace locations, and scanline or window locations is assumed. One can think of the fracture trace pattern as being fixed and the circles as being deployed randomly, with circle centers following a uniform distribution in the plane. Alternatively, circles may be arranged in a regular grid, with the grid located at random relative to the array of fracture traces. In either case, the fundamental assumption of independence is met. No assumptions regarding the trace pattern itself are needed or used, beyond the assumption that statistically homogeneous regions are identified for analysis. For circle sampling in an irregular region, circles can be deployed uniformly in a circumscribed rectangle, and only those circles fully inside the trace observation area retained for analysis (Fig. 4).

2.5. Estimator notation and properties

Estimator notation and terminology used here are consistent with standard statistical usage (e.g. Ang and Tang, 1975). Estimates of mean fracture trace parameters obtained from the circular sampling tools are referred to as point estimates. In this paper, such estimates are denoted with a hat ($^\wedge$). The only exceptions are the (hatless) point estimates n and m (Fig. 2c). In statistical theory, estimates with an expected value equal to the true population mean are referred to as unbiased. Estimates whose expectations asymptote to the true mean are asymptotically unbiased estimates. Of the estimators described in this paper, the
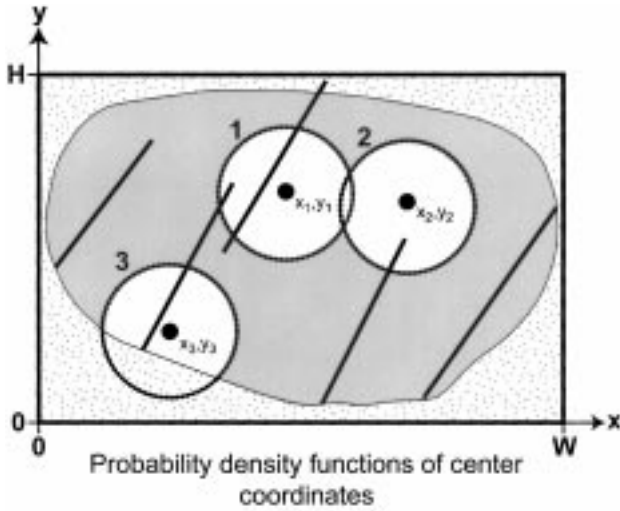
f_x(x) = 1/W for 0 ≤ x ≤ W, = 0 elsewhere

f_y(y) = 1/H for 0 ≤ y ≤ H, = 0 elsewhere

Fig. 4. Circular scanlines/windows with centers (x, y) located independently and at random within an exposure (light grey region). Circles 1 and 2 are acceptable; circle 3 is unacceptable because it lies partly outside the exposed region.

intensity and density estimators are unbiased and the mean trace length estimator is asymptotically unbiased.

3. Intensity estimator

The intensity estimator is based on a count of the number (n) of intersections between fracture traces and one or more circular scanlines (Fig. 2c). This circle-based estimator is known in the field of stochastic geometry (Stoyan et al., 1995). It can be traced to an elegant theorem by Poincaré (see Santaló, 1976), who derived a more general result, which includes circles as a special case, using the technique of differential forms (Schreiber, 1977). The derivation presented here first considers the simple geometry of a set of parallel traces and a single circular scanline, and is subsequently extended to consider multiple sets, traces of variable orientation and multiple circles. The intensity estimator can be derived by several other techniques; perhaps the most direct is to consider the expected number of trace intersections on a randomly oriented straight scanline. The following derivation was chosen because it makes direct use of the measurement tool itself, i.e. a circle.

3.1. Parallel fracture traces

We assume without loss of generality that the traces are parallel to the x-axis (Fig. 5a, b) and restrict our attention initially to the first quadrant of the circle. With the assumed independence between trace and circle locations, the z-coordinate (Fig. 5b) of any trace intersecting the first
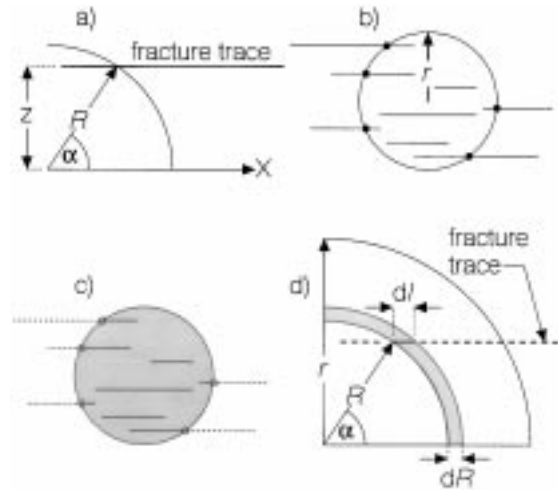

Fig. 5. (a) Position of trace intersect in terms of z-coordinate and angle α between intersection point and x-axis. (b) Parallel traces intersecting a circular scanline of radius r. (c) Visible trace segments (solid) in a circular window of radius r. (d) Differential length dl of trace contained within annulus of width dR and radius R.

quadrant of a circle of radius R is uniformly distributed on $(0, R)$ with probability density function (pdf) $g(z)$ of z given by

$$g(z) = 1/R, \quad 0 < z \leq R, \quad = 0 \quad \text{elsewhere.} \quad (1)$$

Let α denote the acute angle between the x-axis and the radius to the intersection point (Fig. 5a). The pdf $f(\alpha)$ of angle α is found from

$$f(\alpha) = g(z) \left| \frac{\mathrm{d}z}{\mathrm{d}\alpha} \right|, \quad 0 \leq \alpha \leq \pi/2, \quad (2)$$

where $z = R \sin \alpha$, dz/d$\alpha = R \cos \alpha$ and

$$f(\alpha) = (R \cos \alpha)/R = \cos \alpha, \quad 0 \leq \alpha \leq \pi/2. \quad (3)$$

Let $n = n(r)$ denote the number of intersections with a circle of radius r (Fig. 5b), let $\bar{n}(r)$ denote the expectation of n, and let $\bar{n}_Q(r)$ denote the expected number of intersections with the first quadrant, where by symmetry, $\bar{n}_Q(r) = \bar{n}(r)/4$. Similarly, let $L = L(r)$ denote the summed lengths of traces and parts of traces contained inside the circular scanline (Fig. 5c), let $\bar{L}(r)$ denote the expectation of L, and let $\bar{L}_Q(r)$ denote the expected total length in the first quadrant where, by symmetry, $\bar{L}_Q(r) = \bar{L}(r)/4$.

In order to relate $\bar{n}_Q(r)$ to $\bar{L}_Q(r)$, we integrate trace length in the first quadrant. A trace intersecting the circle at angle α has differential length d$l = \sec\alpha$ dR inside a differential annulus of radius R (Fig. 5d). Then

$$\bar{L}_Q(r) = \int_{R=0}^{r} \int_{\alpha=0}^{\pi/2} \bar{n}_Q(R)\sec \alpha f(\alpha) \, \mathrm{d}\alpha \, \mathrm{d}R$$

$$= \int_{R=0}^{r} \int_{\alpha=0}^{\pi/2} \bar{n}_Q(R) \, \mathrm{d}\alpha \, \mathrm{d}R \quad = \frac{\pi}{2} \int_{0}^{r} \bar{n}_Q(R) \, \mathrm{d}R \quad (4)$$

and the expectation of total trace length in the entire circle is

$$\bar{L} = 4\bar{L}_Q = \frac{\pi}{2} \int_0^r 4\bar{n}_Q(R) \, dR = \frac{\pi}{2} \int_0^r \bar{n}(R)dR. \tag{5}$$

Dividing both sides by the area of the circle,

$$I = \frac{1}{2r^2} \int_0^r \bar{n}(R) \, dR, \tag{6}$$

where I is the fracture trace intensity (mean length of traces per unit area). Since areal intensity is independent of the shape and size of the measurement region, the right-hand side of Eq. (6) must be independent of r, implying that the integral in Eq. (6) is proportional to r^2, and that

$$\bar{n}(R) = cR, \tag{7}$$

where c is a constant. Substitution of Eq. (7) into Eq. (6) followed by integration of Eq. (6) shows that $c = 4I$. Substituting this value of c into Eq. (7), and replacing the mean $\bar{n}$ with the point estimate n, we obtain, for a circle of radius r,

$$\hat{I} = \frac{n}{4r}, \tag{8}$$

where $\hat{I}$ is an unbiased estimator for trace intensity.

3.2. Fracture traces of variable orientation

Natural fracture patterns may comprise a variety of orientations, or indeed single traces may be curved. To cope with variable trace orientations we simply need note that intensities are additive; the total intensity of an array of traces is the sum of the intensities of its constituent sets. Formally, we subdivide trace orientations in the range $[0, \pi]$ into k non-overlapping intervals $\Delta\theta_i$, $i = 1, 2, ..., k$, with mean orientations θ_i and magnitudes π/k. Let $I(\theta_i)$ denote the intensity of traces with orientations in the range $\Delta\theta_i$ and let $E[n(\theta_i)]$ denote the expected number of intersections of traces with orientations in the range $\Delta\theta_i$ with the circular scanline of radius r. Then for each interval $i = 1, 2, ..., k$, the x-axis can be re-oriented so as to coincide with θ_i and we have the approximate result,

$$I(\theta_i) \approx \frac{E[n(\theta_i)]}{4r}, \tag{9}$$

the approximation being due to the range of angles in the interval $\Delta\theta_i$. Proceeding to the limit (letting $k \rightarrow \infty$), the relation becomes exact and

$$I = \sum_{i=1}^k I(\theta_i) = \frac{1}{4r} \sum_{i=1}^k E[n(\theta_i)] = \frac{\bar{n}}{4r}, \tag{10}$$

where $\bar{n}$ is the mean total count of intersections on the circular scanline. The intensity estimator $n/4r$ is thus valid regardless of the orientation distribution of the fracture traces.

3.3. Multiple circular scanlines

Several circular scanlines may be deployed to obtain an improved intensity estimate, and indeed, this practice is recommended. If the circles are all the same size, n counts are determined for each circle and then averaged, since r is constant, for substitution into Eq. (8). If circles of different radii are used, the individual point estimates of n are weighted by their respective perimeters to determine an average intensity. Thus, if circles of radius r_1, r_2, ..., r_k, with perimeters p_1, p_2, ..., p_k yield counts n_1, n_2, ..., n_k and intensity estimates I_1, I_2, ..., I_k, the length-weighted intensity estimate is

$$\hat{I} = \frac{\hat{I}_1 p_1 + \hat{I}_2 p_2 + ... + \hat{I}_k p_k}{p_1 + p_2 + ... + p_k} = \frac{2\pi(\hat{I}_1 r_1 + \hat{I}_2 r_2 + ... + \hat{I}_k r_k)}{2\pi(r_1 + r_2 + ... + r_k)}$$

$$= \frac{1}{4} \frac{n_1 + n_2 + ... + n_k}{r_1 + r_2 + ... + r_k} = \frac{\bar{n}}{4\bar{r}}. \tag{11}$$

4. Density estimator

The density estimator uses circular windows rather than circular scanlines, and makes use of the association between trace ends and trace centers. The latter are unidentifiable for censored traces. To illustrate the association between ends and centers, we begin by imagining fracture traces as randomly polarized, each with a positive and a negative end, and we suppose that the window contains $m(+)$ positive and $m(-)$ negative ends (Fig. 3). A one-to-one correspondence exists between positive ends and trace centers, and also between negative ends and trace centers. Trace ends of either polarity could therefore be used to estimate trace density. A better, maximum sample approach is to use an average of the two, yielding for a window of area A, an unbiased density estimator given by

$$\hat{\rho} = \frac{1}{2} \left(\frac{m(+)}{A} + \frac{m(-)}{A} \right) = \frac{m}{2A}, \tag{12}$$

where m is the total number of trace endpoints in the window. As shown in Mauldon (1998), the above principle is valid for any shape window, whether convex or not. For a circular window of radius r (Fig. 2c), the unbiased density estimator $\hat{\rho}$ is

$$\hat{\rho} = \frac{m}{2\pi r^2}. \tag{13}$$

4.1. Multiple circular windows

When several circular windows are used to obtain a single density estimate, the combined circle area can be treated as a single non-convex window. From Eq. (12), the unbiased density estimator $\hat{\rho}$ for multiple windows, valid even if the
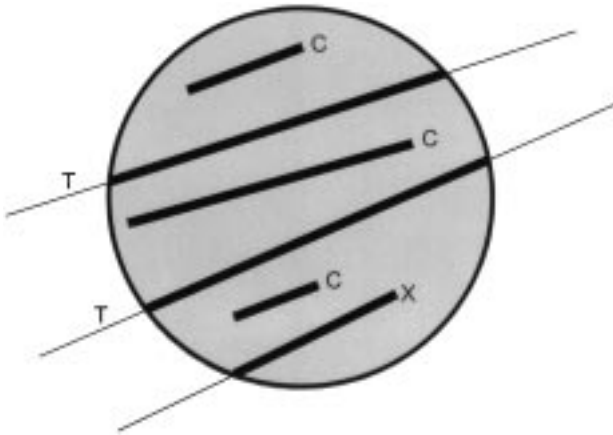
Fig. 6. Intersections (indicated by bold line segments) between fracture traces and circular window. C: trace *contained* entirely within the window (uncensored). T: trace *transects* completely across the window (doubly censored). X: one end only terminates within the window (singly censored).
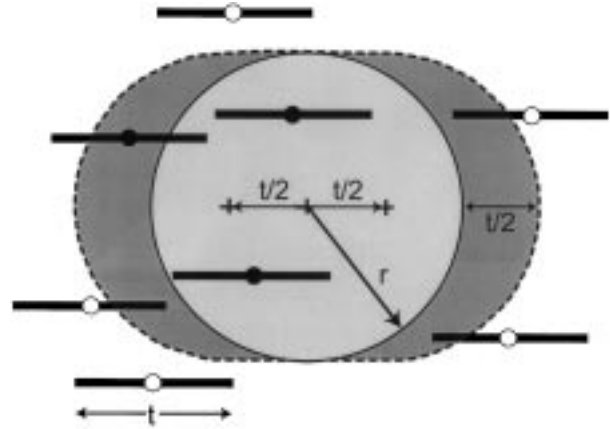

Fig. 7. Locus of trace centers (combined shaded area) for intersection between traces of fixed length and orientation, and circular window of radius r. Traces with centers marked by white dots do not intersect the window.

circles overlap, is

$$\hat{\rho} = \frac{1}{2\pi}\left(\frac{\Sigma m}{\Sigma r^2}\right). \tag{14}$$

5. Mean trace length estimator

The mean trace length estimator considers the intersections (which in this case are line segments) of traces with circular windows (Fig. 6), as well as the intersections (points) of traces with circular scanlines (Fig. 2c). The three types of intersection between traces and a circular window are shown in Fig. 6. Following Pahl (1981), a trace is said to be *contained* in a window if the entire trace is inside the window, and to *transect* the window if the trace is doubly censored, i.e. cuts across and extends beyond the window. The third possibility is *one-end-in* (Cruden, 1977), where traces are singly censored. All six of the traces shown in Fig. 6 *intersect* the circular window.

The estimator derived here is an extension of a method used by Pahl (1981) for parallel traces in a rectangular window. The circle-based estimator (Mauldon, 1998; Zhang and Einstein, 1998) is a special case of a mean trace length estimator developed for convex windows of arbitrary shape (Mauldon, 1998). We first establish the relation between the number of traces that intersect the window, on average, and the trace density and mean trace length. Let N denote the number of traces that intersect a window, where intersection may take any of the variety of forms shown in Fig. 6, and let $N|t, \theta$ denote the number of traces with length t and orientation θ that intersect the window.

Considering only traces of length t and orientation θ, the locus of trace centers for intersection is found as the union of the circular window of radius r and two circular disks, also of radius r, translated a distance $t/2$ in directions θ and

$-\theta$, respectively (Fig. 7). Fracture traces of length t and orientation θ will intersect the window if and only if their centers fall within this combined region (shaded in Fig. 7). The areas of the lune-shaped regions (shaded dark in Fig. 7) to the left and right of the circular window are each equal to the product of width $t/2$ and height $2r$ (Mauldon, 1998). Therefore, the total area $A(t)$ of the shaded region in Fig. 7 is

$$A(t) = \pi r^2 + 2rt. \tag{15}$$

Because of the circular symmetry of the window, $A(t)$ is independent of angle θ and thus the expectation of N conditioned on t is given by

$$E(N|t) = E\left(N|\ t, \theta\right) = \rho\left(\pi r^2 + 2rt\right), \tag{16}$$

where, as before, ρ is the density of trace centers. For an arbitrary cumulative distribution function (cdf) F of trace length t, we now have

$$E(N) = \int_{t=0}^{t=\infty} E(N|\ t)\, \mathrm{d}F(t) = \rho \int_0^1 \left(\pi r^2 + 2rt\right) \mathrm{d}F$$

$$= \rho\pi r^2 \int_0^1 \mathrm{d}F + 2r\rho \int_0^1 t\,\mathrm{d}F. \tag{17}$$

The integral $\int_0^1 \mathrm{d}F$ is equal to unity and the integral $\int_0^1 t\,\mathrm{d}F$ is equal to the mean of t for an arbitrary cdf F of t (Feller, 1971). Thus,

$$\bar{N} = E(N) = \rho\pi r^2 + 2r\rho\mu, \tag{18}$$

where μ is the mean trace length. Riemann–Stieltjes integration, in which the cumulative distribution function F, rather than the trace length t, is used as the variable of integration, has been used in Eq. (17) to cover all distributions F of trace length, whether continuous, discrete or mixed (Loève, 1960). If t has a continuous distribution with probability density function $f(t)$, one can make the substitution $\mathrm{d}F(t) = f(t)\mathrm{d}t$. If t has a discrete distribution

with probability mass function $p(t)$, one can make the substitution $dF(t) = p(t)$ and replace the integral with a summation.

Since the population density ρ and the mean $\bar{N}$ of N are fixed (albeit unknown) quantities, and not random variables, Eq. (18) can be solved for mean trace length μ to give

$$\mu = \frac{1}{2r}\left(\frac{\bar{N}}{\rho}\right) - \frac{\pi r}{2}. \tag{19}$$

As before, let m denote the number of trace endpoints inside the circular window and let n denote the number of intersections between traces and the bounding circular scanline (Fig. 2c). Also, let $\hat{N}$ denote the total number of traces observed to intersect the window, let $\hat{N}_C$ denote the number of traces that are contained in the window and let $\hat{N}_T$ denote the number of traces that transect the window (Fig. 6). Then,

$$n = (\hat{N} - \hat{N}_C - \hat{N}_T) + 2\hat{N}_T = \hat{N} - \hat{N}_C + \hat{N}_T, \tag{20}$$

$$m = (\hat{N} - \hat{N}_C - \hat{N}_T) + 2\hat{N}_C = \hat{N} + \hat{N}_C - \hat{N}_T \tag{21}$$

and, adding the above two equations,

$$\hat{N} = \frac{n + m}{2}. \tag{22}$$

Taking $\hat{N} = (n + m)/2$ and $\hat{\rho} = m/(2\pi r^2)$ as point estimates of $\bar{N}$ and ρ, from Eqs. (22) and (13), respectively, we obtain, from substitution of these quantities into Eq. (19),

$$\hat{\mu} = \frac{1}{2r}\left(\frac{\hat{N}}{\hat{\rho}}\right) - \frac{\pi r}{2} = \frac{1}{2r}\left(\frac{n+m}{2}\right)\left(\frac{2\pi r^2}{m}\right) - \frac{\pi r}{2}, \tag{23}$$

which reduces to the mean trace length estimator,

$$\hat{\mu} = \frac{\pi r}{2}\left(\frac{n}{m}\right). \tag{24}$$

5.1. Multiple circles

The numbers n and m in Eq. (24) are point estimates of the population means $\bar{n}$ and $\bar{m}$, i.e. the average n count and the average m count on circles of radius r. Lower variance estimates of $\bar{n}$ and $\bar{m}$ can be obtained from larger samples. One way to achieve larger sample size is to use several circles. If several circles of the same size are used, n counts and m counts must be obtained separately for each circle (rather than recording the ratio n/m for each circle). The n counts and the m counts are each summed and averaged, and the ratio of these averages is used in the mean trace length estimator,

$$\hat{\mu} = \frac{\pi r}{2}(\bar{n}/\bar{m}). \tag{25}$$

It is important to note that the ratio of the averages, as in Eq. (25), is quite different from the average $\overline{n/m}$ of the ratios, use of which can lead to highly erroneous estimates of mean trace length. For mean trace length estimates using multiple

circles of different size, appropriate average n counts and m counts should be determined using Eqs. (11) and (14), respectively, for substitution into Eq. (25).

6. A unified set of fracture trace parameters

As was mentioned in Section 2, trace intensity is the product of trace density and mean trace length if the two are uncorrelated. We now show that the estimators for these parameters obey the same relationship. Taking the product of the density estimator (Eq. (13)) and the mean trace length estimator (Eq. (24)), we find that

$$\hat{\rho} \times \hat{\mu} = \frac{m}{2\pi r^2} \times \frac{\pi r}{2}\left(\frac{n}{m}\right) = \frac{n}{4r} = \hat{I}, \tag{26}$$

which is the intensity estimator given by Eq. (8).

7. Estimator performance

7.1. Synthetic fracture patterns

Estimates of trace intensity, density and mean trace length obtained from the new circle-based estimation tools were tested against known characteristics of a variety of synthetic trace patterns generated via Monte Carlo simulation (Rohrbaugh et al., 2001, in review). Fig. 8 shows results obtained from sampling synthetic fracture traces in a square analysis region (Gilmour et al., 1986) of edge 100 units, using 50 randomly placed circles of radius 10. The length unit is arbitrary. Estimates of fracture trace intensity, density and mean trace length based on the new circle-based tools fluctuate about the known input values for the synthetic population, while their running means approach the population values as sample size increases (Fig. 8), thus validating the new estimation tools.

Also shown in Fig. 8 are direct estimates from areal samples. Intensity estimates determined by summing trace length in circular areas of radius 10 are virtually indistinguishable (Fig. 8a) from results obtained using the circular scanline intensity estimator (Eq. (8)). Therefore, since counting points on a circular scanline takes significantly less time than measuring the enclosed trace lengths, one can conclude that circular scanlines are a more efficient means for estimating trace intensity than areal sampling.

Systematic errors occur, however, with direct areal estimates (apparent measures) of density and mean trace length. Apparent density (Fig. 8b) overestimates population density by a factor of 3 or more, whereas apparent mean trace length (Fig. 8c) underestimates population mean trace length by a factor of 11. In contrast, estimates from the new estimation tools (Eqs. (13) and (24)) converge on the true input values (Fig. 8b, c). Increasing sample area reduces censoring and improves the performance of the apparent measures. Apparent measures based on the entire square region, for example, give significantly better results than
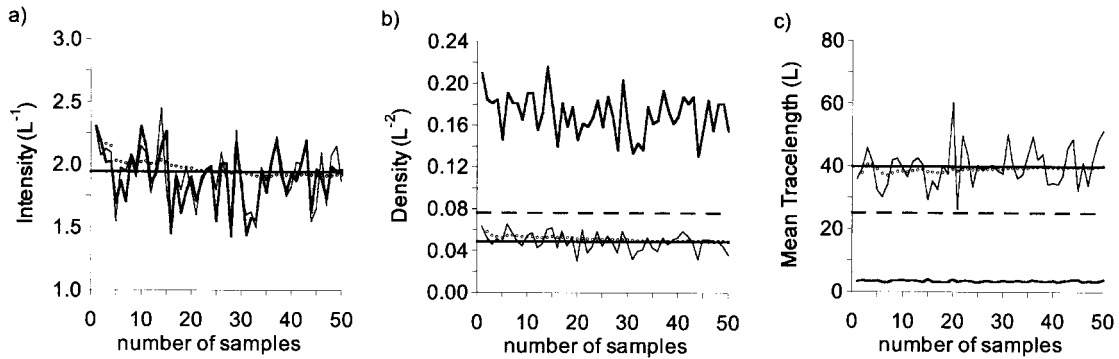
Fig. 8. Application of new circle-based estimators (Eqs. (8), (13) and (24)) to a synthetic population of fracture traces with known geometric parameters. Jagged black lines: new estimators; open circles: running averages of new estimators; horizontal black lines: input parameters; grey lines: areal (apparent) estimates using the circular windows; dashed lines: areal (apparent) estimates from entire analysis region. (a) Intensity (actual value = 1.95 L^{-1}). (b) Density (actual value = 0.051 L^{-2}). (c) Mean trace length (input lengths uniformly distributed from 20 to 60 L; input orientations uniformly distributed from 030° to 090°).

apparent measures based on the circular windows (Fig. 8b, c). The whole-sample apparent measures are still inferior, however, to estimates obtained from using the new tools with just one circle (Fig. 8b, c). Consequently, it is reasonable to conclude that the new estimators perform much better than the apparent measures when estimating density and mean trace length for a fracture trace population.

7.2. Natural pavement at Llantwit Major

The Llantwit Major pavement (Rohrbaugh et al., 2000) contains two orthogonal fracture sets (Fig. 9). The older master joints, which strike 165°, mostly transect the pavement and are therefore doubly censored. The shorter younger cross joints, which strike 075°, typically terminate at master joints, creating an overall ladder geometry for the two sets together (Hancock, 1985).

For estimating trace intensity at Llantwit Major, circular scanline estimates, on average, closely match the areal intensity measures for each of the two sets (Fig. 10a, d). Circular scanlines with $r > 1$ m slightly underestimate the average intensity, however, because due to their size, these larger circles are restricted to the NW, less intensely fractured portion of the pavement (Fig. 9). The circular scanlines, in this case, detect spatial variation in intensity that is averaged out by sampling the entire area.

The circle-based density estimate (0.35 m^{-2}, based on the 2-m circle) of the master joints at Llantwit Major was much less than the measured apparent density (3.4 m^{-2}; Fig. 10b). The circle-based mean trace length estimate (8.7 m, based on a weighted average of the 2-m circle results), on the other hand, was significantly greater than the apparent mean trace length (2.2 m) of the master joints (Fig. 10c). Having in the previous section demonstrated the lack of bias of the new estimators using Monte Carlo simulation, we interpret the circle-based estimates as being representative of the true population values, and the apparent measures as being significantly in error for these highly censored master

joint traces. Benefits from using the new techniques for measuring density and mean trace length of the cross joints at Llantwit Major were minor, however, due to the short lengths of the cross joints in relation to the pavement area and the corresponding lack of censoring and length bias (Figs. 9 and 10e, f).

Further corroboration of these new tools for the characterization of fracture traces is shown in Fig. 11, which is a field photograph looking along the strike of the master joints
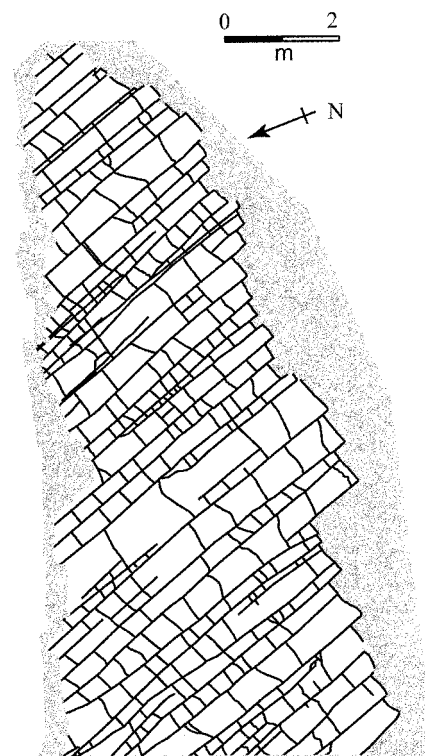

Fig. 9. Fracture trace network on a Jurassic limestone bedding surface at Llantwit Major, Wales (British National Grid location SS95756754). Pavement area is 49.5 m^2, total trace length is 266 m, number of master joints is 75, and number of cross joints is 298.
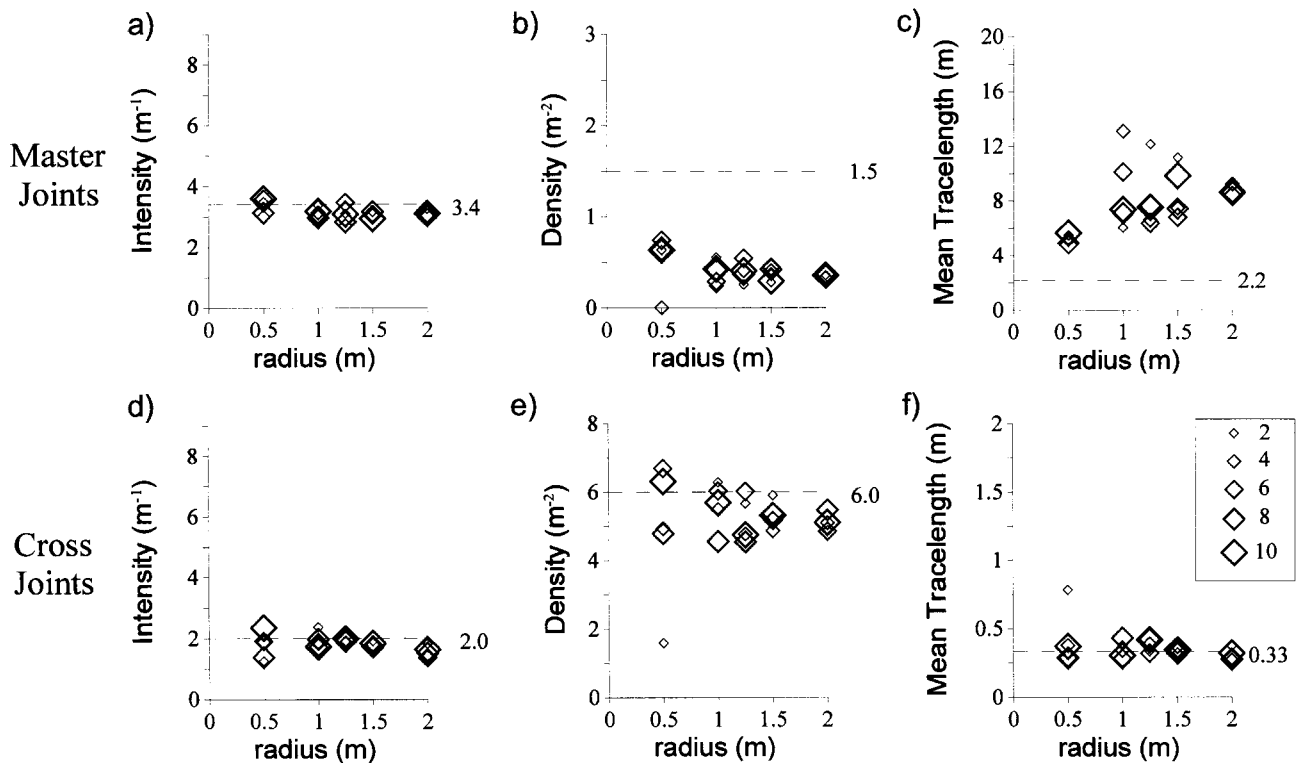
Fig. 10. Fracture trace parameters at Llantwit Major estimated by circular scanlines/windows (diamonds) vs. areal sampling of entire pavement (numbers, dashed lines). Master joints: (a) intensity; (b) density; (c) mean trace length. Cross joints: (d) intensity; (e) density; (f) mean trace length.

on a larger nearby pavement at Llantwit Major. Cursory examination of the master joints in this photograph reveals a range of trace lengths with a mean significantly longer than the apparent mean of 2.2 m and probably longer than the maximum recorded trace length of 6.2 m (Fig. 8). The traces visible in Fig. 11 appear to have a mean that more
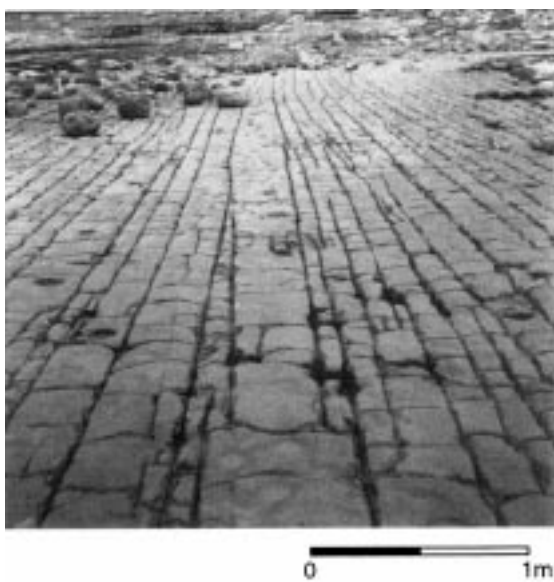

Fig. 11. Master joints on limestone bed at Llantwit Major, Wales. View north, adjacent to mapped pavement. Scale is approximate.

closely corresponds to the estimate of 8.7 m obtained using the new circle-based estimation tools.

8. Discussion and conclusions

Advantages of the new trace intensity, density and mean trace length estimators include the following. (1) The estimators are very simple, as they require only counts of circle–trace intersections and trace endpoints. (2) The estimation tools can be rapidly deployed either on actual rock surfaces or on images thereof, using either low-tech equipment such as chalk and string, or computer technology. (3) Because of the circular symmetry of the new sampling tools, the estimators eliminate orientation bias in the plane. (4) Using methods from geometrical probability, the new estimators automatically correct for the problems of censoring and length bias that plague other approaches to determination of trace characteristics. (5) The estimators measure a unified self-consistent set of geometric trace parameters. (6) These new tools may be applied to other populations of lines, including, for example, lineations and fault arrays, as well as temporal data sets.

Cautions and limitations include the following. (1) The estimators presented here are applicable only to populations and not to single features. (2) The estimators do not capture aggregate properties such as transmissive pathways, termination types and network style. (3) The methods presented

here, as with any scanline or areal sampling technique, are applicable to the fracture traces on a 2-d surface, and not directly to the 3-d fracture system. With respect to this last point, it should be noted that relationships between 2-d traces and 3-d fractures have received considerable attention in the rock engineering literature (e.g. Warburton, 1980a,b), although the problems are by no means solved. One simple approach to inferring 3-d fracture properties, unfortunately not always applicable, is to deploy these new tools on three orthogonal rock surfaces.

Acknowledgements

References

Ang, A.H-S., Tang, W.H., 1975. Probability Concepts in Engineering Planning and Design, Vol. 1. John Wiley, New York.

Baecher, G.B., 1980. Progressively censored sampling of rock joint traces. Mathematical Geology 12, 33–40.

Baecher, G.B., Lanney, N.A., 1978. Trace length biases in joint surveys. Proceedings of the 19th US Symposium on Rock Mechanics, Lake Tahoe, Nevada, 1, pp. 56–65.

Becker, A., Gross, M.R., 1996. Mechanism for joint saturation in mechanically layered rocks: an example from southern Israel. Tectonophysics 257, 223–237.

Call, R.D., Savely, J.P., Nicolas, D.E., 1976. Estimation of joint set characteristics from surface mapping data. In: Hustrulid, W.A. (Ed.), Monograph on Rock Mechanics Applications in Mining, AIME, New York, pp. 65–73.

Cruden, D.M., 1977. Describing the size of discontinuities. International Journal of Rock Mechanics and Mining Sciences and Geomechanical Abstracts 14, 133–137.

Davis, G.H., Reynolds, S.J., 1996. Structural Geology of Rocks and Regions, John Wiley, New York, pp. 724–726.

Dershowitz, W.S., Einstein, H.H., 1988. Characterizing rock joint geometry with joint system models. Rock Mechanics and Rock Engineering 21, 21–51.

Dershowitz, W.S., Herda, H.H., 1992. Interpretation of fracture spacing and intensity. In: Tillerson, J.R., Wawersik, W.R. (Eds.), Proceedings of the 33rd US Symposium on Rock Mechanics, Balkema, Rotterdam, pp. 757–766.

Dershowitz, W.S, Follin, S., Mauldon, M., 2000. Fracture intensity measures in 1-D, 2-D, and 3-D at Äspö, Sweden, Proceedings of the 4th North American Rock Mechanics Symposium, Pacific Rocks 2000, in press.

Epstein, B., 1954. Truncated life tests in the exponential case. Annals of Mathematics and Statistics 25, 555.

Feller, W., 1971. An Introduction to Probability Theory and its Applications. 2nd ed., Wiley, New York.

Gilmour, H.M.P., Billaux, D., Long, J.C.S, 1986. Models for calculating fluid flow in randomly generated three-dimensional networks of disk-shaped fractures: theory and design of FMG3D, DISCEL and DIMES. Lawrence Berkeley Laboratory, Earth Sciences Division, LBL-19515.

Hancock, P.L., 1985. Brittle microtectonics; principles and practice. Journal of Structural Geology 7, 437–457.

Kulatilake, P.H.S.W., Wu, T.H., 1984a. The density of discontinuity traces in sampling windows. International Journal of Rock Mechanics and Mining Sciences and Geomechanical Abstracts 21, 345–347.

Kulatilake, P.H.S.W., Wu, T.H., 1984b. Estimation of mean trace length of discontinuities. Rock Mechanics and Rock Engineering 17, 215–232.

LaPointe, P.R., 1993. Pattern analysis and simulation of joints for rock engineering. In: Hudson, J.A. (Ed.), Comprehensive Rock Engineering, Vol. 3: Rock Testing and Site Characterization, Pergamon Press, New York, pp. 215–239.

Laslett, G.M., 1982. Censoring and edge effects in areal and line transect sampling of rock joint traces. Mathematical Geology 14, 125–139.

Loève, M., 1960. Probability Theory, 2nd ed. Van Nostrand, Princeton.

Maritz, J.S., 1981. Distribution-free Statistical Methods. Chapman & Hall, London.

Mauldon, M., 1994. Intersection probabilities of impersistent joints. International Journal of Rock Mechanics and Mining Sciences and Geomechanical Abstracts 31, 107–115.

Mauldon, M., 1998. Estimating mean fracture trace length and density from observations in convex windows. Rock Mechanics and Rock Engineering 31, 201–216.

Mauldon, M., Mauldon, J.G., 1997. Fracture sampling on a cylinder: from scanlines to boreholes and tunnels. Rock Mechanics and Rock Engineering 30, 129–144.

Mauldon, M., Rohrbaugh Jr., M.B., Dunne, W.M., Lawdermilk, W., 1999a. Fracture intensity estimates using circular scanlines. In: Amadei, B., Kranz, R.L., Scott, G.A., Smeallie, P.H. (Eds.), Proceedings of the 37th US Rock Mechanics Symposium: Rock Mechanics for Industry, Balkema, Rotterdam, pp. 777–784.

Mauldon, M., Rohrbaugh Jr., M.B., Dunne, W.M., Lawdermilk, W., 1999b. Estimators for mean fracture trace length and density using circular windows. In: Amadei, B., Kranz, R.L., Scott, G.A., Smeallie, P.H. (Eds.), Proceedings of the 37th US Rock Mechanics Symposium: Rock Mechanics for Industry, Balkema, Rotterdam, pp. 785–792.

Mecke, J., 1981. Formulas for stationary planar fibre processes. III. Intersections with fibre systems. Mathematische Operationsforschung und Statistik, Series Statistik 12, 201–210.

Oda, M., 1993. Modern developments in rock structure characterization. In: Hudson, J.A. (Ed.), Comprehensive Rock Engineering, Vol. 1, Pergamon Press, New York, pp. 185–200.

Odling, N.E., 1997. Scaling and connectivity of joint systems in sandstones from western Norway. Journal of Structural Geology 19, 1257–1271.

Pahl, P.J., 1981. Estimating the mean length of discontinuity traces. International Journal of Rock Mechanics and Mining Sciences and Geomechanical Abstracts 18, 221–228.

Panek, L.A., 1985. Estimating fracture trace length from censored measurements of multiple scanlines. In: Stephansson, O. (Ed.), Proceedings of the International Symposium on Fundamentals of Rock Joints, Centek, Bjorkliden, pp. 13–23.

Parker, P., Cowan, R., 1976. Some properties of line segment processes. Journal of Applied Probability 13, 96–107.

Pollard, D.D, Aydin, A., 1988. Progress in understanding jointing over the past century. Geological Society of America Bulletin 100, 1181–1204.

Priest, S.D., 1993. Discontinuity Analysis for Rock Engineering. Chapman & Hall, New York.

Priest, S.D., Hudson, J.A., 1981. Estimation of discontinuity spacing and trace length using scanline surveys. International Journal of Rock Mechanics and Mining Sciences and Geomechanics Abstracts 18, 183–197.

Rohrbaugh Jr., M.B., Mauldon, M., Dunne, W.M., 2001, in review. Estimating joint intensity, density and mean tracelength using circular scanlines and circular windows. American Association of Petroleum Geologist Bulletin (in press).

Santaló, L.A., 1976. Integral Geometry and Geometric Probability. Addison-Wesley, Reading, MA.

Schreiber, M., 1977. Differential Forms: A Heuristic Introduction. Springer, New York.

Stoyan, D., Kendall, W.S., Mecke, J., 1995. Stochastic Geometry and its Applications, 2nd ed. John Wiley, New York, pp. 286–296.

Terzaghi, R.D., 1965. Sources of error in joint surveys. Geotechnique 15, 287–304.

Titley, S.R., Thompson, R.C., Haynes, F.M., Manske, S.L., Robison, L.C., White, J.L., 1986. Evolution of fractures and alteration in the Sierrita-Esperanza Hydrothermal System, Pima County, Arizona. Economic Geology 81, 343–370.

Underwood, A.E., 1970. Quantitative Stereology. Addison-Wesley, Reading, MA.

Villaescusa, E., Brown, E.T., 1992. Maximum Likelihood estimation of joint size from trace length measurements. Rock Mechanics and Rock Engineering 25, 67–87.

Warburton, P.M., 1980a. A stereological interpretation of joint trace data. International Journal of Rock Mechanics and Mining Sciences and Geomechanics Abstracts 17, 181–190.

Warburton, P.M., 1980b. Stereological interpretation of joint trace data: influences of joint shape and implications for geological surveys. International Journal of Rock Mechanics and Mining Sciences and Geomechanics Abstracts 17, 305–316.

Wu, H., Pollard, D.D., 1995. An experimental study of the relationship between joint spacing and layer thickness. Journal of Structural Geology 17, 887–905.

Zhang, L., Einstein, H.H., 1998. Estimating the mean trace length of rock discontinuities. Rock Mechanics and Rock Engineering 31, 217–234.